Dynamic Analysis by Meshless Local Petrov-Galerkin Formulations Considering a Time-Marching Scheme Based on Implicit Green's Functions

D. Soares Jr.[1], J. Sladek[2] and V. Sladek[2]

Abstract: In recent years the idea of using mesh-free or mesh-less methods for numerical solution of partial differential equations has received much attention, due to their potential advantage in eliminating the costly effort of mesh generation and re-meshing. A variety of meshless methods has been proposed so far. Many of them are derived from a weak-form formulation on global domain or a set of local subdomains. In the global formulation background cells are required for the integration of the weak form. In methods based on local weak-form formulation no cells are required and therefore they are often referred to as truly meshless methods. If for the geometry of subdomains a simple form is chosen, numerical integrations can be easily carried out over them. The meshless local Petrov-Galerkin (MLPG) method is a fundamental base for the derivation of many meshless formulations, since trial and test functions are chosen from different functional spaces. In the present paper, the MLPG is applied to solve linear and nonlinear dynamic 2-D problems. Both the Heaviside step function and the Gaussian weight function are used as the test functions in the local weak form to investigate which one is more convenient. The moving least square (MLS) method is used for approximation of physical quantities in the local integral equations. After spatial discretization, a system of ordinary differential equations of second order for unknown nodal quantities is obtained. A time-marching scheme which is based on implicit Green's functions is applied to solve this system of equations in the time domain. In this procedure, the time-domain Green's matrices of the elastodynamic problem are considered in order to generate a recursive relationship to evaluate displacements and velocities at each time-step. Taking into account the Newmark method, the Green's matrices of the problem are numerically and implicitly evaluated, establishing the Green-Newmark method. At the end of the work, numerical examples are presented, verifying the

[1] Structural Engineering Department, Federal University of Juiz de Fora, CEP 36036-330 Juiz de Fora, MG, Brazil. Phone: +55 32 2102 3468. E-mail: delfim.soares@ufjf.edu.br

[2] Institute of Construction and Architecture, Slovak Academy of Sciences, 84503 Bratislava, Slovakia. E-mail: usarslad@savba.sk

accuracy and potentialities of the new methodology.

Keywords: Dynamics, Meshless Local Petrov-Galerkin, Moving Least Squares Interpolation, Green-Newmark Method, Time-Domain Analysis, Elastoplastic Analysis.

1   Introduction

In recent years, meshless methods have become very popular computational tools for many engineering problems. This is due to their high adaptivity and low costs to prepare input and output data for numerical analyses. The moving least-squares (MLS) approximation is generally considered as one of many schemes to interpolate discrete data with a reasonable accuracy [Belytschko et al. (1996); Atluri and Shen (2002); Atluri (2004)]. The order of continuity of the MLS approximation is given by the minimum between the orders of continuity of the basis functions and that of the weight function. This allows the order of continuity to be tuned to a desired value. In conventional discretization methods, such as the Finite Element Method (FEM) or the Boundary Element Method (BEM), the interpolation functions usually result in a discontinuity of secondary fields (gradients of primary fields) on the interfaces of elements. Therefore, modeling based on C^1-continuity, such as in meshless methods, is expected to be more accurate than conventional discretization techniques.

The meshless method can be obtained from a weak-form formulation on either the global domain or a set of local subdomains. In the global formulation, background cells are required for the integration of the weak-form [Belytschko et al. (1994)]. In methods based on local weak-form formulation [Zhu et al. (1998), Atluri and Zhu (1998)], no background cells are required and therefore they are often referred to as truly meshless methods. The meshless local Petrov-Galerkin (MLPG) method is a fundamental base for the derivation of many meshless formulations since the trial and test functions can be chosen from different functional spaces. Recent successes of MLPG methods have been reported in the development of the MLPG finite-volume mixed method [Atluri et al. (2004)], which was later extended to finite deformation analysis of static and dynamic problems [Han et al. (2005)]; in simplified treatment of essential boundary conditions by a novel modified MLS procedure [Gao et al. (2006)]; and in the development of the mixed scheme to interpolate the elastic displacements and stresses independently [Atluri et al. (2006)].

The possibility of selecting arbitrary test functions in the weak formulation allows the derivation of many computational methods based on the MLPG in elastodynamics [Sellountos and Polyzos (2003); Sellountos et al. (2005, 2009); Vavourakis et al. (2006)]. In an early stage of the MLPG, the fundamental solution has been

used as the test function. It led to accurate numerical results and it was utilized in former papers for isotropic homogeneous and continuously nonhomogeneous bodies under static [Atluri et al. (2000), Sladek et al. (2000)] and dynamic loads [Sladek et al. (2003a,b)]. In these formulations, Green's functions which vanish on the local boundary of a circular subdomain were successfully utilized. However, in anisotropic elasticity, the fundamental solution is too complex or unavailable in a closed form. Starting from a complex fundamental solution, it is very difficult to derive the Green's function that vanishes on the local boundary of a subdomain. Hence, the local integral equations involving such fundamental solutions as the test functions are computationally inconvenient, since both the displacements and tractions are unknown on the boundary of the interior sub-domain and the number of integrals is doubled. Therefore, it is convenient to use the Gaussian weight function or the Heaviside step function as the test functions on circular subdomains, leading to a general approach with high applicability to a wide class of problems. Batra and Ching (2002) applied the MLPG with Gaussian weight functions to elastodynamic problems. The MLPG method with a Heaviside step function as the test functions [Atluri and Shen (2002), Atluri et al. (2003)] has been applied to solve two-dimensional homogeneous and continuously non-homogeneous elastic problems [Sladek et al., (2004; 2009), (2008a)], thermoelastic problems [Sladek et al., (2006)], and for 3-D problems in homogeneous and isotropic solids under a static or a dynamic load [Han and Atluri (2004a,b), Sladek et al. (2009)]. The present authors have recently analyzed 3-D axisymmetric dynamic problems in continuously non-homogeneous elastic solids [Sladek et al. (2005), (2008b)]. Recently, Long et al. (2008) applied the MLPG to elasto-plastic problems under a stationary load and Soares et al. (2009b) analyzed dynamic elasto-plastic models by the MLPG.

The weak form on local subdomains, considering the Gaussian weight function or the Heaviside step function as the test function, is employed here to derive the local integral equations. The integral equations have a very simple nonsingular form. Moreover, both the contour and domain integrations can be easily carried out on circular sub-domains.

Regarding time dependent analysis, Laplace transform formulations or time-domain formulations are usually employed. Laplace transform formulations are less accurate for large instants due to the instability of the Laplace inversion. Time-domain formulations, on the other hand, are usually based in a time-marching procedure, which is very appropriate to carry out nonlinear analysis. In the present work, a time-marching scheme, based on implicit Green's functions, is discussed. This time-domain approach, as is described along the text, is easy to implement, accurate, unconditionally stable and it avoids the iterative procedures which are usually related to the dynamic analysis of elasto-plastic models.

Dynamic analysis by implicit Green's functions was firstly presented by Soares (2002, 2004), taking into account linear and nonlinear models discretized by the finite element method. Later on, the methodology was extended, taking into account not only time-domain numerical procedures to evaluate the Green's matrices (Soares and Mansur, 2005a), but also Laplace and frequency-domain numerical procedures (Soares and Mansur, 2005b; Loureiro and Mansur, 2009a). The technique was also applied associated to other numerical procedures, such as the boundary element method (Soares, 2007) and the finite difference method (Mansur et al., 2007); and to analyse coupled problems, such as fluid-structure, soil-structure and electromagnetic interaction problems, taking into account FEM-BEM coupling procedures (Soares and Mansur, 2005c; Soares et al., 2007; Soares, 2009), and pore-dynamics problems, taking into account finite element procedures (Soares, 2008). Recently, the methodology has been applied to analyse heat conduction models (Mansur et al., 2009; Loureiro et al., 2009; Loureiro and Mansur, 2009b), extrapolating the context of wave propagation problems initially focused.

2   Governing equations

The basic equations related to the dynamic modelling in focus are given by:

$$\sigma_{ij,j} - \rho\,\ddot{u}_i + \rho\,b_i = 0 \tag{1}$$

$$d\varepsilon_{ij} = \tfrac{1}{2}(du_{i,j} + du_{j,i}) \tag{2}$$

$$d\sigma_{ij} = D^*_{ijkl}\,d\varepsilon_{kl} = D_{ijkl}\,d\varepsilon_{kl} - d\sigma^*_{ij} \tag{3}$$

where equation (1) is the equilibrium equation and equations (2) and (3) stand for incremental relations. The cauchy stress, using the usual indicial notation for cartesian axes, is represented by σ_{ij}, and u_i and b_i stand for displacement and body force distribution components, respectively. Inferior commas and overdots indicate partial space and time derivatives, respectively, and ρ stands for the mass density. The incremental strain components $d\varepsilon_{ij}$ are defined in the usual way from the displacements, as described by equation (2). Equation (3) is the constitutive law, written incrementally. D^*_{ijkl} is a tangential tensor defined by suitable state variables and the direction of the increment. In the particular case of linear elastic analysis, equation (3) can be rewritten as $\sigma_{ij} = D_{ijkl}\,\varepsilon_{kl}$, and the constitutive tensor D_{ijkl} is given by:

$$D_{ijkl} = 2\mu\nu/(1-2\nu)\,\delta_{ij}\delta_{kl} + \mu\,(\delta_{ik}\delta_{jl} + \delta_{il}\delta_{jk}) \tag{4}$$

where μ and ν stand for the shear modulus and the Poisson ratio of the model, respectively, and δ_{ij} represents the Kronecker delta ($\delta_{ij} = 0$ if $i \neq j$ and $\delta_{ij} = 1$ if

$i = j$). In the present work, linear elastic analyses are firstly focused, being non-linear elastoplastic analyses discussed in section 5, by the introduction of pseudo-forces (in this case, the pseudo-forces are computed based on the non-linear stresses σ_{ij}^*).

In addition to equations (1)-(3), boundary and initial conditions have to be prescribed in order to completely define the problem. they are given as follows:

(i) Boundary Conditions ($t \geq 0$, $\mathbf{x} \in \Gamma$ Where $\Gamma = \Gamma_u \cup \Gamma_\tau$):

$$u_i = \bar{u}_i \text{ for } \mathbf{x} \in \Gamma_u \tag{5a}$$

$$\tau_i = \sigma_{ij} \cdot n_j = \bar{\tau}_i \text{ for } \mathbf{x} \in \Gamma_\tau \tag{5b}$$

(ii) Initial Conditions ($t = 0$, $\mathbf{x} \in \Omega$):

$$u_i = \bar{u}_i^0 \tag{6a}$$

$$\dot{u}_i = \dot{\bar{u}}_i^0 \tag{6b}$$

where the prescribed values are indicated by over bars and τ_i stands for traction components along the boundary whose unit outward normal vector is represented by n_i. The boundary of the model is denoted by Γ and the domain by Ω.

3   Spatial discretization

In the present text, first the spatial discretization by meshless techniques is described and, once the time-domain matricial equation is obtained, its temporal discretization is discussed (section 4). In general, a meshless method uses a local interpolation to represent the trial function with the values (or the fictitious values) of the unknown variable at some randomly located nodes. The moving least squares (MLS) approximation may be considered as one of such schemes, and it is employed here. Once the trial function is established, it can be applied to a generalized local weak form of the equations described in section 2, and the mass and stiffness matrix of the method can be deduced. In subsection 3.1, the moving least square approximation is described, whereas in subsection 3.2 the spatially discretized matricial equation is presented. Two MLPG formulations are discussed here, namely the MLPG formulation with Gaussian weight functions as text functions, and the MLPG formulation with Heaviside step functions as text functions.

3.1   *Moving least squares approximation*

Consider a sub-domain Ω_x, the neighbourhood of a point $\mathbf{x}$ and denoted as the domain of definition of the MLS approximation for the trial function at $\mathbf{x}$, which is

located in the problem domain Ω. To approximate the distribution of function u_i in Ω_x, over a number of randomly located nodes, the MLS approximantion u_i^h of u_i, can be defined by [Atluri and Shen (2002)]:

$$u_i^h(\mathbf{x},t) = \mathbf{\Phi}^T(\mathbf{x})\hat{\mathbf{u}}_i(t) = \sum_{a=1}^{N} \phi^a(\mathbf{x})\hat{u}_i^a(t) \tag{7}$$

where $\hat{u}_i$ is the fictitious nodal value of u_i (N is the number of points in the sub-domain Ω_x) and the shape matrix $\mathbf{\Phi}^T(\mathbf{x})$ is defined by:

$$\mathbf{\Phi}^T(\mathbf{x}) = \mathbf{p}^T(\mathbf{x})\mathbf{A}^{-1}(\mathbf{x})\mathbf{B}(\mathbf{x}) \tag{8}$$

where

$$\mathbf{A}(\mathbf{x}) = \sum_{a=1}^{N} w^a(\mathbf{x})\mathbf{p}(\mathbf{x}^a)\mathbf{p}^T(\mathbf{x}^a) \tag{9a}$$

$$\mathbf{B}(\mathbf{x}) = [w^1(\mathbf{x})\mathbf{p}(\mathbf{x}^1), w^2(\mathbf{x})\mathbf{p}(\mathbf{x}^2), ..., w^N(\mathbf{x})\mathbf{p}(\mathbf{x}^N)] \tag{9b}$$

and $\mathbf{p}^T(\mathbf{x}) = [p_1(\mathbf{x}), p_2(\mathbf{x}), \ldots, p_m(\mathbf{x})]$ is a complete monomial basis of order m. $w^a(\mathbf{x})$ is the weight function associated with node a. The gaussian weight function is adopted here, and it is given by:

$$w^a(\mathbf{x}) = \frac{\exp[-(d_a/c_a)^{2k}] - \exp[-(r_a/c_a)^{2k}]}{1 - \exp[-(r_a/c_a)^{2k}]}(1 - H[d_a - r_a]) \tag{10}$$

where $d_a = ||\mathbf{x} - \mathbf{x}^a||$ is the distance between the sampling point $\mathbf{x}$ and node $\mathbf{x}^a$, c_a is a constant controlling the shape of the weight function and r_a is the radius of the circular support of the weight function. The Heaviside unit step function is defined as $H(z) = 1$ for $z > 0$ and $H(z) = 0$ for $z \leq 0$. The size of the weight function support should be large enough to have a sufficient number of nodes covered in the domain of definition to ensure the regularity of matrix $\mathbf{A}$.

3.2 *Local weak-form discretization*

Instead of writing the global weak-form for the governing equations described in section 2, the MLPG method constructs a weak-form over local fictitious subdomains, such as Ω_s, which is a small region taken for each node inside the global domain (see Fig.1). The local sub-domains overlap each other, and cover the whole global domain Ω. The geometrical shape and size of the local sub-domains can be arbitrary. In the present paper, the local sub-domains are taken to be of circular
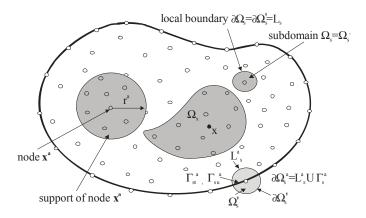
Figure 1: Local boundaries and the MLS approximation of trial functions around node $\mathbf{x}^a$.

shape. The local weak-form of the governing equations described in section 2 can be written as:

$$
\int_{\partial\Omega_s} \sigma_{ij}n_j u_{ik}^* d\Gamma - \int_{\Omega_s} \sigma_{ij} u_{ik,j}^* d\Omega + \int_{\Omega_s} (-\rho\,\ddot{u}_i + \rho\,b_i)\,u_{ik}^* d\Omega + \lambda \int_{\Gamma_{su}} (u_i - \bar{u}_i)\,u_{ik}^* d\Gamma = 0
$$

(11)

where u_{ik}^* is a test function and λ is a penalty parameter, which is introduced here in order to impose essential prescribed boundary conditions in an integral form. $\partial\Omega_s$ is the boundary of the local sub-domain, which consists of three parts $\partial\Omega_s = L_s \cup \Gamma_{s\tau} \cup \Gamma_{su}$, in general. Here, L_s is the local boundary that is totally inside the global domain, $\Gamma_{s\tau}$ is the part of the local boundary which coincides with the global traction boundary, i.e., $\Gamma_{s\tau} = \partial\Omega_s \cap \Gamma_\tau$, and, similarly, Γ_{su} is the part of the local boundary that coincides with the global displacement boundary, i.e., $\Gamma_{su} = \partial\Omega_s \cap \Gamma_u$ (see Fig.1).

Equation (11) can be simplified according to the chosen test function u_{ik}^*. By specifying the local sub-domain as the circle Ω^c centred at node $\mathbf{x}^c$ and by choosing a test function which provides null spatial derivatives in each sub-domain, such as the Heaviside step function $u_{ik}^* = \delta_{ik}(1 - H(d_c - r_c))$, the local weak-form (11) can

then be converted into the following local boundary-domain integral equation:

$$\sum_{a=1}^{N}\left[\left(\int_{\Omega^c}\rho\phi^a d\Omega\right)\ddot{\hat{\mathbf{u}}}^a - \left(\lambda\int_{\Gamma_u^c}\phi^a d\Gamma + \int_{L^c+\Gamma_u^c}\mathbf{NDB}^a d\Gamma\right)\hat{\mathbf{u}}^a\right] =$$

$$= \int_{\Gamma_\tau^c}\bar{\boldsymbol{\tau}}\,d\Gamma + \int_{\Omega^c}\rho\mathbf{b}\,d\Omega - \lambda\int_{\Gamma_u^c}\bar{\mathbf{u}}d\Gamma \quad (12a)$$

where, for the development of the above equation, definition (7) is employed and Voigt notation (i.e., $\boldsymbol{\sigma} = [\sigma_{11}, \sigma_{22}, \sigma_{12}]^T$, $\tau = [\tau_1, \tau_2]^T$, $\mathbf{u} = [u_1, u_2]^T$ etc.) is considered.

On the other hand, by choosing a test function with vanishing value on the local boundary that is totally inside the global domain, such as the Gaussian weight function $u_{ik}^* = \delta_{ik}w^c$, one can rewrite equation (11) into the local integral equation:

$$\sum_{a=1}^{N}\left[\left(\int_{\Omega^c}w^c\rho\phi^a d\Omega\right)\ddot{\hat{\mathbf{u}}}^a - \left(\lambda\int_{\Gamma_u^c}w^c\phi^a d\Gamma + \int_{\Gamma_u^c}w^c\mathbf{NDB}^a d\Gamma - \int_{\Omega^c}\mathbf{W}^c\mathbf{DB}^a d\Omega\right)\hat{\mathbf{u}}^a\right]$$

$$= \int_{\Gamma_\tau^c}w^c\bar{\boldsymbol{\tau}}\,d\Gamma + \int_{\Omega^c}w^c\rho\mathbf{b}\,d\Omega - \lambda\int_{\Gamma_u^c}w^c\bar{\mathbf{u}}d\Gamma \quad (12b)$$

where, for both equations (12a) and (12b), matrices $\mathbf{N}$, $\mathbf{W}^a$, $\mathbf{B}^a$ and $\mathbf{D}$ are given by:

$$\mathbf{N} = \begin{bmatrix} n_1 & 0 & n_2 \\ 0 & n_2 & n_1 \end{bmatrix} \quad (13a)$$

$$\mathbf{W}^a = \begin{bmatrix} w_{,1}^a & 0 & w_{,2}^a \\ 0 & w_{,2}^a & w_{,1}^a \end{bmatrix} \quad (13b)$$

$$\mathbf{B}^a = \begin{bmatrix} \phi_{,1}^a & 0 \\ 0 & \phi_{,2}^a \\ \phi_{,2}^a & \phi_{,1}^a \end{bmatrix} \quad (13c)$$

$$\mathbf{D} = \begin{bmatrix} D_{1111} & D_{1122} & D_{1112} \\ D_{1122} & D_{2222} & D_{2212} \\ D_{1112} & D_{2212} & D_{1212} \end{bmatrix} = \frac{2\mu}{1-2\nu} \begin{bmatrix} 1-\nu & \nu & 0 \\ \nu & 1-\nu & 0 \\ 0 & 0 & (1-2\nu)/2 \end{bmatrix} \quad (13d)$$

By collecting all nodal unknown fictitious displacements $\hat{\mathbf{u}}^a(t)$ into vector $\hat{\mathbf{U}}(t)$, the system of the discretized equations (12a) or (12b) can be rewritten into matrix form, as follows:

$$\mathbf{M}\ddot{\hat{\mathbf{U}}}(t) + \mathbf{K}\hat{\mathbf{U}}(t) = \mathbf{F}(t) \quad (14)$$

where $\mathbf{M}$ is the mass matrix, evaluated taking into account the first integral term in the l.h.s. of equations (12), $\mathbf{K}$ is the stiffness matrix, computed regarding the remaining terms on the l.h.s. of equations (12), and $\mathbf{F}$ is the external load vector, evaluated considering the terms on the r.h.s. of equations (12).

Once the ordinary differential matrix equation (14) is established, its solution in the time-domain is discussed in the next section, taking into account the Green-Newmark time-marching procedure.

4   Temporal discretization

By solving the time-domain second-order ordinary differential equation (14) analytically, the following expressions for the displacement and velocity fictitious vectors may be obtained:

$$\hat{\mathbf{U}}(t) = \dot{\mathbf{\Lambda}}(t)\,\mathbf{M}\,\hat{\mathbf{U}}^0 + \mathbf{\Lambda}(t)\,\mathbf{M}\,\dot{\hat{\mathbf{U}}}^0 + \mathbf{\Lambda}(t) \bullet \mathbf{F}(t) \tag{15a}$$

$$\dot{\hat{\mathbf{U}}}(t) = \ddot{\mathbf{\Lambda}}(t)\,\mathbf{M}\,\hat{\mathbf{U}}^0 + \dot{\mathbf{\Lambda}}(t)\,\mathbf{M}\,\dot{\hat{\mathbf{U}}}^0 + \dot{\mathbf{\Lambda}}(t) \bullet \mathbf{F}(t) \tag{15b}$$

where $\mathbf{\Lambda}(t)$ represents the Green's function matrix of the model and the symbol $\bullet$ stands for time convolution.

The jth column of $\mathbf{\Lambda}(t)$ can be obtained through the solution of equation (14) for an impulsive load applied at node j or by taking into account the physical identity: "*impulse = momentum variation*". In this last case, the Green's function matrix $\mathbf{\Lambda}(t)$ can be directly evaluated by considering equation (14) associated to an initial condition problem, where $\mathbf{\Lambda}(0) = \mathbf{0}$ and $\dot{\mathbf{\Lambda}}(0) = \mathbf{M}^{-1}$.

In the present work, the fictitious displacements and velocities of the model are evaluated employing equations (15) and the Green's matrices are calculated numerically and implicitly, taking into account the above-mentioned initial condition problem and usual time-domain integration procedures (namely, the Newmark method – Newmark, 1959).

Equations (15), at time Δt, read:

$$\hat{\mathbf{U}}(\Delta t) = \dot{\mathbf{\Lambda}}(\Delta t)\,\mathbf{M}\,\hat{\mathbf{U}}^0 + \mathbf{\Lambda}(\Delta t)\,\mathbf{M}\,\dot{\hat{\mathbf{U}}}^0 + \int_0^{\Delta t} \mathbf{\Lambda}(\Delta t - \tau)\,\mathbf{F}(\tau)\,d\tau \tag{16a}$$

$$\dot{\hat{\mathbf{U}}}(\Delta t) = \ddot{\mathbf{\Lambda}}(\Delta t)\,\mathbf{M}\,\hat{\mathbf{U}}^0 + \dot{\mathbf{\Lambda}}(\Delta t)\,\mathbf{M}\,\dot{\hat{\mathbf{U}}}^0 + \int_0^{\Delta t} \dot{\mathbf{\Lambda}}(\Delta t - \tau)\,\mathbf{F}(\tau)\,d\tau \tag{16b}$$

Assuming that Δt is small enough, the following approximation can replace the integrals indicated in equations (16):

$$\int_0^{\Delta t} g(\Delta t - \tau) f(\tau) d\tau = g(0) f(\Delta t) \Delta t \tag{17}$$

where $g(t)$ and $f(t)$ are two generic time functions. Equation (17) may seem over simplified, however, it is the result one reaches if a discrete frequency-domain approach is considered [Soares and Mansur, 2003]. Moreover, as it has been shown [Soares and Mansur, 2005a], approximation (17) applied to equations (16) is equivalent to a two-point Newton-Cotes quadrature rule, for most usual engineering problems. In the present work, equation (17) is adopted since it provides accurate results for most applications and it is efficient and extremely easy to implement (although many other expressions are possible).

Taking into account equations (16), with the approximations indicated by equation (17), recursive expressions can be obtained by considering equations (15) at time $t + \Delta t$ and by supposing that the analysis begins at time t. The recurrence relations that arise are given by:

$$\hat{\mathbf{U}}^{t+\Delta t} = \dot{\mathbf{\Lambda}}(\Delta t) \mathbf{M} \hat{\mathbf{U}}^t + \mathbf{\Lambda}(\Delta t) \mathbf{M} \dot{\hat{\mathbf{U}}}^t + \mathbf{\Lambda}(0) \mathbf{F}^{t+\Delta t} \Delta t \tag{18a}$$

$$\dot{\hat{\mathbf{U}}}^{t+\Delta t} = \ddot{\mathbf{\Lambda}}(\Delta t) \mathbf{M} \hat{\mathbf{U}}^t + \dot{\mathbf{\Lambda}}(\Delta t) \mathbf{M} \dot{\hat{\mathbf{U}}}^t + \dot{\mathbf{\Lambda}}(0) \mathbf{F}^{t+\Delta t} \Delta t \tag{18b}$$

where, as mentioned before, the Green's matrices $\mathbf{\Lambda}(\Delta t)$, $\dot{\mathbf{\Lambda}}(\Delta t)$ and $\ddot{\mathbf{\Lambda}}(\Delta t)$ are evaluated by solving the following initial condition problem, at time instant Δt:

$$\mathbf{M}\ddot{\mathbf{\Lambda}}(t) + \mathbf{K}\mathbf{\Lambda}(t) = \mathbf{0} \tag{19a}$$

where

$$\mathbf{\Lambda}(0) = \mathbf{0} \tag{19b}$$

$$\dot{\mathbf{\Lambda}}(0) = \mathbf{M}^{-1}. \tag{19c}$$

In the present work, the Newmark method is employed to solve the initial condition problem (19); nevertheless, many other methodologies are possible. The expressions for $\mathbf{\Lambda}^{\Delta t}$, $\dot{\mathbf{\Lambda}}^{\Delta t}$ and $\ddot{\mathbf{\Lambda}}^{\Delta t}$ given by the Newmark method read:

$$\mathbf{\Lambda}^{\Delta t} = (1/(\alpha \Delta t))(\mathbf{K} + (1/(\alpha \Delta t^2))\mathbf{M})^{-1} \tag{20a}$$

$$\dot{\mathbf{\Lambda}}^{\Delta t} = (\gamma/(\alpha \Delta t))\mathbf{\Lambda}^{\Delta t} - (1 - \gamma/\alpha)\mathbf{M}^{-1} \tag{20b}$$

$$\ddot{\mathbf{\Lambda}}^{\Delta t} = (1/(\alpha\Delta t^2))\mathbf{\Lambda}^{\Delta t} - (1/(\alpha\Delta t))\mathbf{M}^{-1} \tag{20c}$$

where α and γ are the Newmark's parameters.

Substituting equations (20) into the recurrence relations (18), taking into account equations 19(b) and 19(c), one finally obtains:

$$\hat{\mathbf{U}}^{t+\Delta t} = \mathbf{\Pi}(c_1\hat{\mathbf{U}}^t + c_2\dot{\hat{\mathbf{U}}}^t) + c_3\hat{\mathbf{U}}^t \tag{21a}$$

$$\dot{\hat{\mathbf{U}}}^{t+\Delta t} = \mathbf{\Pi}(c_4\hat{\mathbf{U}}^t + c_1\dot{\hat{\mathbf{U}}}^t) - c_2\hat{\mathbf{U}}^t + c_3\dot{\hat{\mathbf{U}}}^t + \mathbf{R}^{t+\Delta t} \tag{21b}$$

where

$$\mathbf{\Pi} = (\mathbf{K} + (1/(\alpha\Delta t^2))\mathbf{M})^{-1}\mathbf{M} \tag{22a}$$

$$\mathbf{R}^{t+\Delta t} = \mathbf{M}^{-1}\mathbf{F}^{t+\Delta t}\Delta t \tag{22b}$$

and

$$c_1 = \gamma/(\alpha^2\Delta t^2) \tag{23a}$$

$$c_2 = 1/(\alpha\Delta t) \tag{23b}$$

$$c_3 = 1 - \gamma/\alpha \tag{23c}$$

$$c_4 = 1/(\alpha^2\Delta t^3) \tag{23d}$$

Equations (21) are the final recurrence relations for the Green-Newmark algorithm. As it has been described [Soares and Mansur, 2005a; Soares 2007], the Green-Newmark method provides stable and accurate results in the sense that the crucial modes are accurately integrated and the spurious modes are filtered out. In the next subsection, the stability and numerical dispersion of the proposed time-marching technique is further discussed.

4.1 Stability analysis

Taking into account a one degree-of-freedom problem, equation (14) can be rewritten as

$$\ddot{\hat{U}}(t) + w^2\hat{U}(t) = F(t) \tag{24}$$

where w is the natural frequency of the model. A recursive relationship can be established, regarding the Green-Newmark method applied to equation (24), as follows:

$$\begin{bmatrix} \hat{U}^{t+\Delta t} \\ \dot{\hat{U}}^{t+\Delta t} \end{bmatrix} = \begin{bmatrix} A_{11} & A_{12} \\ A_{21} & A_{22} \end{bmatrix} \begin{bmatrix} \hat{U}^t \\ \dot{\hat{U}}^t \end{bmatrix} + \begin{bmatrix} L_1 \\ L_2 \end{bmatrix} = \mathbf{A} \begin{bmatrix} \hat{U}^t \\ \dot{\hat{U}}^t \end{bmatrix} + \mathbf{L} \tag{25}$$

where $\mathbf{A}$ is the amplification matrix and $\mathbf{L}$ is the load operator vector. The entries of matrix $\mathbf{A}$ are given by:

$$A_{11} = A_{22} = 1 - (\Delta t^2 w^2 \gamma)/(\Delta t^2 w^2 \alpha + 1) \tag{26a}$$

$$A_{12} = -A_{21}/w^2 = \Delta t/(\Delta t^2 w^2 \alpha + 1) \tag{26b}$$

which, as one can observe, provides the same values as the standard Newmark method if the trapezoidal rule (i.e., $\alpha = 1/4$ and $\gamma = 1/2$) is adopted. If different choices for parameters α and γ are considered, the Green-Newmark and the standard Newmark methods become different procedures. In the present work, one group of possible choices for parameters α and γ is focused, namely: $\gamma = 1/2$ and $\alpha > \gamma/2$. This group is selected since, in the Newmark method, unconditional stable algorithms are conditioned by $2\alpha \geq \gamma \geq 1/2$ and second order accuracy is achieved if and only if $\gamma = 1/2$.
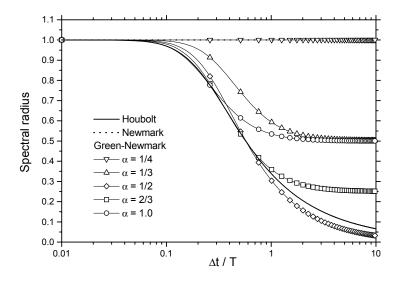

Figure 2: Spectral radius for the Houbolt, Newmark and Green-Newmark methods ($\gamma = 1/2$ and $\alpha \geq \gamma/2$).

In order to take a closer look at the numerical properties of the Green-Newmark method, the spectral radius of the amplification matrix $\mathbf{A}$ is analyzed. In Fig.2, the relations $\rho(\mathbf{A}) \, x \, \Delta t/T$ are depicted, where $\rho(\mathbf{A})$ is the spectral radius of matrix $\mathbf{A}$ and T is the natural period of the problem (one should observe that, for the standard Newmark method, $\rho(\mathbf{A}) = 1.0$ once $\gamma = 1/2$ and $\alpha \geq \gamma/2$ are selected). For unconditional stable algorithms, the relation $\rho(\mathbf{A}) \leq 1.0$ must hold.

As one can observe, numerical damping is introduced by the Green-Newmark method. This numerical damping is usually less expressive than that introduced by the Houbolt method [Houbolt, 1950] (it depends on the time discretization adopted) and always (for the focused choice of parameters α and γ) more expressive than that regarding the standard Newmark method. This property is beneficial to MLPG formulations since it allows the elimination of spurious modes contributions, providing a more robust time-marching technique. As it is illustrated in the first example discussed in section 6, dynamic analyses by MLPG formulations are very sensitive to the influence of spurious modes, and unstable results may often arise if proper time-marching procedures are not considered [Soares et al. (2009a)].

Moreover, as one can observe in equation (21a), the computation of displacements by the Green-Newmark method is explicit, i.e., it only takes into account previous time-step information ($L_1 = 0$ in equation (25)). As a consequence, some non-linear analyses can be carried out without iterative algorithms, rendering more efficient numerical procedures, as it is discussed in the next section.

5   Non-linear analyses

In this section, dynamic elastoplastic analyses are discussed, taking into account the pseudo-force method. This methodology is considered here once, by the Green-Newmark method, displacement evaluations only depend on loads acting in previous time-steps, which allows the computation of the current stress state at once, at each time-step (i.e., without any iterative procedure).

In the next subsection, the basic equations describing elastoplastic models are briefly presented. In the sequence, the pseudo-force method is discussed in accordance with the discretization techniques reported in sections 3 and 4.

5.1   Elastoplastic models

The incremental stress-strain relation, associated to the elastoplastic problem in focus, can be written as indicated by equation (3), where, within the context of the associated isotropic work hardening theory, the tangent constitutive tensor is defined as:

$$D^*_{ijkl} = D_{ijkl} - (1/\psi)D_{ijmn}a_{mn}a_{op}D_{opkl} \tag{27}$$

where D_{ijkl} is defined by equation (4) and

$$a_{kl} = \partial\bar{\sigma}/\partial\sigma_{kl} \tag{28a}$$

$$\psi = a_{ij}D_{ijkl}a_{kl} + H \tag{28b}$$

$$H = \partial \sigma_0 / \partial \bar{\varepsilon}^p \qquad (28c)$$

In equations (28), $\bar{\sigma}$ and $\bar{\varepsilon}^p$ are the equivalent (or effective) stress and plastic strain, respectively, σ_0 is the uniaxial yield stress and H is the plastic-hardening modulus (the current slope of the uniaxial plastic stress-strain curve). Recall that in case of von Mises isotropic strain-hardening material, the tensor of incremental elastoplastic material moduli takes the form $D_{ijkl}^* = D_{ijkl} - (3\mu / (\sigma_0^2 (1 + H/3))) s_{ij} s_{kl}$, where $s_{ij} = \sigma_{ij} - (1/3)\delta_{ij}\sigma_{kk}$ is the stress deviator; and for the case of a perfectly plastic material $H = 0$.

For the initial stress formulation, it is convenient to define a fictitious "elastic" stress increment as follows:

$$d\sigma_{ij}^e = D_{ijkl}d\varepsilon_{kl} \qquad (29)$$

and to rewrite equation (3) as indicated below:

$$d\sigma_{ij} = d\sigma_{ij}^e - d\sigma_{ij}^* \qquad (30)$$

where the "initial" stress increments are computed by:

$$d\sigma_{ij}^* = (1/\psi)D_{ijmn}a_{mn}a_{kl}d\sigma_{kl}^e \qquad (31)$$

which are employed to evaluate the non-linear pseudo-forces, as is described in the next subsection.

5.2   *The pseudo-force method*

Taking into account the discussion presented in subsection 5.1 and considering $d\sigma_{ij} = d\sigma_{ij}^e - d\sigma_{ij}^*$, equations (12) can be rewritten as follows, taking into account an initial stress formulation:

$$\sum_{a=1}^{N}\left[\left(\int_{\Omega^c}\rho\phi^a d\Omega\right)\ddot{\hat{\mathbf{u}}}^a - \left(\lambda\int_{\Gamma_u^c}\phi^a d\Gamma + \int_{L^c+\Gamma_u^c}\mathbf{NDB}^a d\Gamma\right)\hat{\mathbf{u}}^a\right]$$
$$= \int_{\Gamma_\tau^c}\bar{\boldsymbol{\tau}}d\Gamma + \int_{\Omega^c}\rho\mathbf{b}d\Omega - \lambda\int_{\Gamma_u^c}\bar{\mathbf{u}}d\Gamma - \int_{L^c+\Gamma_u^c}\mathbf{N}\sigma^* d\Gamma \quad (32a)$$

$$\sum_{a=1}^{N}\left[\left(\int_{\Omega^c}w^c\rho\phi^a d\Omega\right)\ddot{\hat{\mathbf{u}}}^a - \left(\lambda\int_{\Gamma_u^c}w^c\phi^a d\Gamma + \int_{\Gamma_u^c}w^c\mathbf{NDB}^a d\Gamma - \int_{\Omega^c}\mathbf{W}^c\mathbf{DB}^a d\Omega\right)\hat{\mathbf{u}}^a\right]$$
$$= \int_{\Gamma_\tau^c}w^c\bar{\boldsymbol{\tau}}d\Gamma + \int_{\Omega^c}w^c\rho\mathbf{b}d\Omega - \lambda\int_{\Gamma_u^c}w^c\bar{\mathbf{u}}d\Gamma - \int_{\Gamma_u^c}w^c\mathbf{N}\sigma^* d\Gamma + \int_{\Omega^c}\mathbf{W}^c\boldsymbol{\sigma}^* d\Omega \quad (32b)$$

which, after proper numerical treatment, provides:

$$\mathbf{M}\ddot{\hat{\mathbf{U}}}(t) + \mathbf{K}\hat{\mathbf{U}}(t) = \mathbf{F}(t) + \mathbf{P}(\hat{\mathbf{U}}(t)) \tag{33}$$

where **M, K** and **F** are exactly those described in equation (14), taking into account linear analysis, and **P** stands for the pseudo-forces related to the nonlinear analysis in focus. The entries of vector **P** are evaluated taking into account the last terms on the r.h.s. of equations (32), which are function of the "plastic" stresses and, as a consequence, of the current-time displacements.

Once equation (33) is established, its solution in the time-domain can be carried out as described in section 4, the only difference remaining in the calculus of the effective force (22b), which should also account for the non-linear pseudo-forces **P**.

In resume, the proposed time-marching procedure to analyse dynamic elastoplastic models can be characterized by the following three consecutive steps: (i) computation of displacements $\hat{\mathbf{U}}^{t+\Delta t}$ (see equation (21a)); (ii) computation of effective forces, taking into account pseudo-forces (i.e., $\mathbf{R}^{t+\Delta t} = \mathbf{M}^{-1}(\mathbf{F}^{t+\Delta t} + \mathbf{P}(\hat{\mathbf{U}}^{t+\Delta t}))\Delta t$); (iii) computation of velocities $\dot{\hat{\mathbf{U}}}^{t+\Delta t}$ (see equation (21b)). Since the computation of the displacements does not depend on the pseudo-forces acting at the same time-step, no iterative procedures are necessary, enabling a very efficient methodology.

6 Numerical aspects and applications

In this section three numerical examples are considered, illustrating the potentialities of the proposed techniques. In the first example (linear analysis), a clamped rod is analyzed considering different time-marching procedures, highlighting the stability of the Green-Newmark method. In the second example, the dynamic behavior of a cantilever beam is studied and the obtained results are compared to those provided by the Finite Element Method (FEM). Finally, in the third example, a soil strip is considered and the obtained results are compared to those obtained by the FEM and by a Newmark/Newton-Raphson approach [Soares et al. (2009b)].

The following nomenclature is adopted here, concerning the meshless formulations in focus: (i) MLPG1 denotes the MLPG formulation employing Heaviside test functions; (ii) MLPG2 denotes the MLPG formulation that employs the weight functions as the test functions. Along the following analyses, the radii of the influence domain and of the local subdomain are set to $\alpha_x d_i^3$ and $\alpha_s d_i^1$, respectively, where d_i^3 and d_i^1 are the distances to the third and first nearest points from node i, respectively. In all the applications that follow, $\alpha_x = 4$ is selected. Considering the MLPG1, $\alpha_s = 0.5$ is always adopted and, for the MLPG2, $\alpha_s = 1.0$ is adopted

for the first and second applications, and $\alpha_s = 0.75$ is adopted in the third application. The mass matrix **M** is diagonalized by a row-sum technique ($M_i^{diag} = \sum\limits_{a=1}^{N} M_{ia}$), avoiding the solution of an extra system of equations (see equation (22b)).

6.1 Clamped rod

The present example consists of a rectangular rod submitted to a time Heavisite force, applied at $t = 0\,s$ and kept constant along time [Soares, 2007; Soares et al., 2009a]. In Fig.3 a sketch of the model is depicted, describing the geometry and the boundary conditions of the problem. The physical properties of the rod are given by: $E = 200\,N/m^2$ (Young modulus), $\rho = 1.0\,kg/m^3$ (mass density) and $v = 0$ (Poisson rate; it is adopted null in order to simulate a one-dimensional analysis). The geometry of the rod is defined by: $a = 2\,m$ and $b = 1\,m$. 153 nodes are employed to spatially discretize the rectangular domain, in a regular equally spaced 9x17 (vertical and horizontal, respectively) distribution. The adopted time-step is given by: $\Delta t = 0.003\,s$.
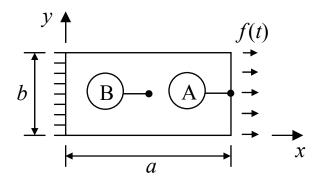

Figure 3: Sketch for the clamped rod: geometry and boundary conditions.

In Fig.4, displacement time-histories at points A ($x = a$, $y = b/2$) and B ($x = a/2$, $y = b/2$) are depicted considering the Houbolt, Newmark and Green-Newmark methods ($\gamma = 1/2$ and $\alpha = 1/2$). As is observed in Fig.4, the Newmark method provides unstable results, whereas stability is observed in the Houbolt and in the Green-Newmark analyses (one should keep in mind, however, that in the Green-Newmark method the introduction of numerical damping can be controlled by selecting appropriate Newmark parameters – the same, on the other hand, is not possible taking into account the Houbolt method).

As can be observed, time-domain analysis of dynamic models discretized by MLPG formulations considering Gaussian weight functions as test functions is more sensi-
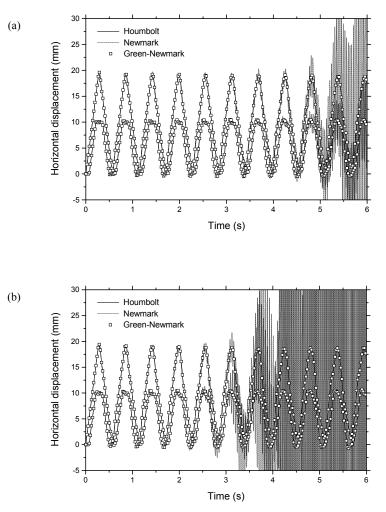
(a)

(b)

Figure 4: Displacement time-history at points A and B considering the Houbolt, Newmark and Green-Newmark methods ($\gamma = 1/2$ and $\alpha = 1/2$): (a) MLPG1; (b) MLPG2.

tive to spurious modes contributions, providing more easily unstable results. MLPG formulations based on Heaviside test functions, on the other hand, not only are more efficient (in terms of computational costs), but also more robust considering time-domain procedures. In both cases, accurate and stable results can be achieved once time-marching procedures with appropriate high-frequency dissipation are considered. It must be noticed that the example in focus is a very important

benchmark since it represents a rather complex numerical computation (in spite of its geometrical and load simplicity) once there are successive reflections occurring at the rod extremities and these multiple reflections can emphasize some numerical aspects, such as instabilities and excessive numerical damping.

6.2 Cantilever beam

This second application consists of a clamped beamlike body [Soares et al., 2009b], subjected to a suddenly applied uniform load (Heaviside time function). A sketch of the model is depicted in Fig.5. The geometry and spatial discretization of the body are the same as in subsection 6.1. The time-step adopted for the analysis is given by: $\Delta t = 0.005\,s$. A perfectly plastic material obeying the von Mises yield criterion is assumed. The physical properties of the model are: $v = 0$, $E = 100\,N/m^2$, $\rho = 1.5\,kg/m^3$ and $\sigma_0 = 0.1\,N/m^2$ (uniaxial yield stress).
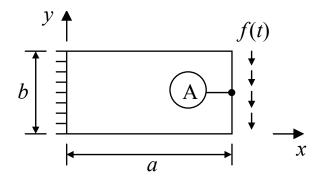

Figure 5: Sketch for the cantilever beam: geometry and boundary conditions.

In Fig.6, time-history results for the vertical displacements at point A ($x = a$, $y = b/2$) are depicted, considering elastic and elastoplastic analyses. Results provided by standard FEM solutions, taking into account the Newmark method (trapezoidal rule) and Newton-Raphson non-linear iterative techniques, are also depicted in Fig.6, for comparison. The FEM analyses take into account two different meshes, namely: (i) Mesh 1 – composed by 128 linear square elements and 153 nodes (located as in the MLPG discretization); (ii) Mesh 2 – composed by 512 linear square elements and 561 nodes. As can be observed, the MLPG results are in good agreement with the FEM results for both linear and non-linear analyses, in spite of its poor spatial discretization.
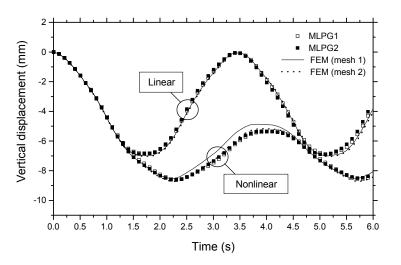
Figure 6: Displacement time-history at point A considering linear and nonlinear analyses by the MLPG (Geen-Newmark method – $\gamma = 1/2$ and $\alpha = 1/2$; 153 nodes) and by the FEM (Newmark method – $\gamma = 1/2$ and $\alpha = 1/4$; mesh 1 with 153 nodes and mesh 2 with 561 nodes).

6.3   Soil strip

In this third example, a two-dimensional soil strip is analysed [Soares et al., 2009b]. A sketch of the model is depicted in Fig.7. A Heaviside time function is considered acting on the strip, as described in Fig.7. The geometry of the model is defined by: $a = 5m$, $b = 5m$ and $c = 0.5m$. 121 nodes are employed to spatially discretize the square domain, in a regular equally spaced 11x11 distribution. The adopted time-step is given by: $\Delta t = 0.001 s$. A perfectly plastic material obeying the Mohr-Coulomb yield criterion is assumed. The physical properties of the model are: $\nu = 0.2$, $E = 10^7 N/m^2$, $\rho = 2 \cdot 10^3 kg/m^3$, $c = 2 \cdot 10^2 N/m^2$ (cohesion) and $\theta = 10^0$ (internal friction angle).

In Fig.8, time-history results for the vertical displacements at point A ($x = 0$, $y = b$) are depicted, considering elastic and elastoplastic analyses. FEM results are also plotted in Fig.8, for comparison. The FEM analyses take into account two different meshes, namely: (i) Mesh 1 – composed by 100 linear square elements and 121 nodes (located as in the MLPG discretization); (ii) Mesh 2 – composed by 400 linear square elements and 441 nodes.

As can be observed, the MLPG results are in good agreement with the FEM results for both linear and non-linear analyses. As is expected, elastoplastic analyses are
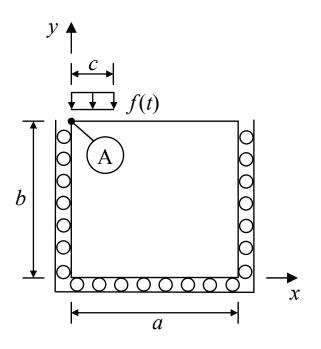
Figure 7: Sketch for the soil strip: geometry and boundary conditions.

greatly influenced by the number of integration points being considered (i.e., by the accuracy in the evaluation of the stresses of the model). Therefore, a richer FEM mesh will provide considerably better results for the non-linear model, as well as the MLPG2 is expected to provide more accurate results than the MLPG1, once more integrations points are employed by the former, due to the domain discretization term in equation (32b). However, also due to this greater amount of integration points in the MLPG2 formulation, its computational costs are considerably higher than those related to the MLPG1, for elastoplastic analysis.

Results obtained by the MLPG considering a Newmark/Newton-Raphson approach [Soares et al., 2009b] are also depicted in Fig.8, for comparison. These results highlight the fact that the Geen-Newmark/Pseudo-force algorithm provides good responses without considering iterative processes, whereas the Newmark/Newton–Raphson approach is far from the correct solution if iterations are not considered.
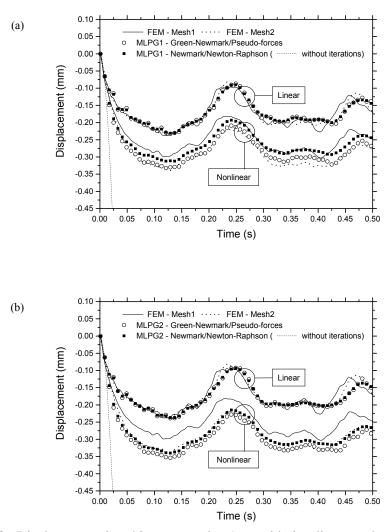
Figure 8: Displacement time-history at point A considering linear and nonlinear analyses by the MLPG (Geen-Newmark/Pseudo-force method – $\gamma = 1/2$ and $\alpha = 1/2$; Newmark/Newton-Raphson method – $\gamma = 0.70$ and $\alpha = 0.36$; 121 nodes) and by the FEM (Newmark/Newton-Raphson method – $\gamma = 0.5$ and $\alpha = 0.25$; mesh 1 with 121 nodes and mesh 2 with 441 nodes): (a) MLPG1; (b) MLPG2.

7 Conclusions

Two MLPG formulations were presented here to analyse the dynamic behaviour of elastic and elastoplastic solids. In the first formulation, Heaviside step func-

tions were adopted as the test functions, eliminating one domain integral of the local weak form equation. In the second formulation, Gaussian weight functions were the considered test functions, allowing eliminating boundary integrals along internal subdomain contours. For both these formulations, a MLS interpolation scheme was adopted, rendering a matricial time-domain system of second order ordinary differential equations. This system was analysed by the implicit Green approach. The implicit Green approach employs a recurrence relationship, to calculate displacements and velocities, which are based on time-domain Green's matrices, numerically and implicitly evaluated. In the present work, these Green's matrices are obtained taking into account the Newmark method, establishing the Green-Newmark algorithm. As it has been shown, the procedure is found stable and accurate, eliminating the spurious oscillatory tendency of the standard Newmark method, and the excessive numerical damping feature of the Houbolt method. The present algorithm also has other advantages, such as: initial conditions are easily considered (in the Houbolt method special initialization procedures must be employed); displacement evaluation only depends on the load acting in previous time-steps, allowing iterative procedures to be eliminated in elastoplastic analysis; it is easy to implement; etc.. As a matter of fact, the time-integration Green method is a wide research field: several numerical procedures may be applied to evaluate (explicitly or implicitly) the Green's matrices of the problem, generating different new methodologies, each one full of potentialities.

It is important to highlight that the adopted meshless techniques give continuous variation of the first or higher order derivatives of the primitive function (in counterpart to classical FEM polynomial approximations where secondary fields have a jump on the interface of elements) and, therefore, more accurate results are expected in dynamic elastoplastic analyses by these techniques, since proper computation of stresses plays a crucial role on these nonlinear models. The MLPG formulation considering the Gaussian weight function as the test function computes the stress states of the model in a large well-distributed number of integration points, allowing a highly accurate evaluation of the internal forces. The MLPG formulation based on Heaviside test functions, on the other hand, provides a computational less expensive numerical procedure, also providing quite accurate results. Moreover, this meshless formulation seems to deal better with the spurious modes related to the dynamic analysis, rendering more stable numerical procedures when considering time-marching schemes.

References

Atluri, S.N. (2004): *The Meshless Method, (MLPG) For Domain & BIE Discretizations*, Tech Science Press.

Atluri, S.N.; Zhu, T. (1998): A New Meshless Local Petrov-Galerkin (MLPG) Approach in Computational Mechanics. *Computational Mechanics*, 22: 117-127.

Atluri, S.N.; Sladek, J.; Sladek, V.; Zhu, T. (2000): The local boundary integral equation (LBIE) and its meshless implementation for linear elasticity. *Comput. Mech.*, 25: 180-198.

Atluri, S.N.; Han, Z.D.; Shen, S.P. (2003): Meshless local Petrov-Galerkin (MLPG) approaches for solving the weakly-singular traction & displacement boundary integral equations. *CMES: Computer Modeling in Engineering & Sciences*, 4: 507-516.

Atluri, S.N.; Shen, S.P. (2002): The meshless local Petrov-Galerkin (MLPG) method: A simple & less costly alternative to the finite element and boundary element methods. *CMES: Computer Modeling in Engineering & Sciences*, 3: 11-51.

Atluri, S.N.; Shen, S.P. (2002): *The Meshless Local Petrov-Galerkin (MLPG) Method*, 440 pages, Tech Science Press.

Atluri, S.N., Han, Z.D., Rajendran, A.M. (2004): A new implementation of the meshless finite volume method, through the MLPG "Mixed" approach. *CMES: Computer Modeling in Engineering & Sciences*, **6**: 491-513.

Atluri, S.N., Liu, H.T., Han, Z.D. (2006): Meshless local Petrov-Galerkin (MLPG) mixed finite difference method for solid mechanics. *CMES: Computer Modeling in Engineering & Sciences*, **15**: 1-16.

Batra, R.C., Ching, H.K. (2002): Analysis of elastodynamic deformations near a crack/notch tip by the meshless local Petrov-Galerkin (MLPG) method. *CMES: Computer Modeling in Engineering & Sciences*, **3**: 717-730.

Belytschko, T., Lu, Y., L. Gu, L. (1994): Element free Galerkin methods, *International Journal for Numerical Methods in Engineering*, **37**, 229-256.

Belytschko, T.; Krogauz, Y.; Organ, D.; Fleming, M.; Krysl, P. (1996): Meshless methods; an overview and recent developments. *Comp. Meth. Appl. Mech. Engn.*, 139: 3-47.

Gao, L., Liu, K., Liu, Y. (2006): Applications of MLPG method in dynamic fracture problems. *CMES: Computer Modeling in Engineering & Sciences*, **12**: 181-195.

Han, Z.D.; Atluri, S.N. (2004a): Meshless local Petrov-Galerkin (MLPG) approaches for solving 3D problems in elasto-statics. *CMES: Computer Modeling in Engineering & Sciences*, 6: 169-188.

Han, Z.D.; Atluri, S.N. (2004b): A meshless local Petrov-Galerkin (MLPG) approach for 3-dimensional elasto-dynamics. *CMC: Computers, Materials & Continua*, 1: 129-140.

Han, Z.D., Rajendran, A.M., Atluri, S.N. (2005): Meshless Local Petrov-Galerkin (MLPG) approaches for solving nonlinear problems with large deformations and rotations. *CMES: Computer Modeling in Engineering & Sciences*, **10**: 1-12.

Houbolt, J.C. (1950): A Recurrence Matrix Solution for the Dynamic Response of Elastic Aircraft, *Journal of the Aeronautical Sciences*, **17**, 540-550.

Long, S.Y., Liu, K.Y., Li, G.Y. (2008): An analysis for the elasto-plastic fracture problem by the meshless local Petrov-Galerkin method. *CMES: Computer Modeling in Engineering & Sciences*, **28**: 203-216.

Loureiro, F. S., Mansur, W. J. (2009a): An efficient hybrid time-Laplace domain method for elastodynamic analysis based on the explicit Green's approach. *International Journal of Solids and Structures*, **46**: 3096-3102.

Loureiro, F. S., Mansur, W. J. (2009b): A new family of time integration methods for heat conduction problems using numerical Green's functions. *Computational Mechanics*, **44**: 519-531.

Loureiro, F. S., Mansur, W. J., Vasconcellos, C. A. B. (2009): A hybrid time/Laplace integration method based on numerical Green's functions in conduction heat transfer. *Computer Methods in Applied Mechanics and Engineering*, **198**: 2662-2672.

Mansur, W. J., Loureiro, F. S., Soares Jr., D., Dors, C. (2007): Explicit time-domain approaches based on numerical Green s functions computed by finite differences The ExGA family. *Journal of Computational Physics*, **227**: 851-870.

Mansur, W. J., Vasconcellos, C. A. B., Zambrozuski, N. J. M., Rotunno Filho, O. C. (2009): Numerical solution for the linear transient heat conduction equation using an Explicit Green's Approach. *International Journal of Heat and Mass Transfer*, **52**: 694-701.

Newmark, N.M. (1959): A method of computation for structural dynamics. *ASCE Journal of Engineering Mechanics Division*, **85**: 67-94.

Sellountos, E.J.; Polyzos, D. (2003): A MLPG (LBIE) method for solving frequency domain elastic problems. *CMES: Computer Modeling in Engineering & Sciences*, 4: 619-636.

Sellountos, E.J.; Vavourakis, V.; Polyzos, D. (2005): A new singular/hypersingular MLPG (LBIE) method for 2D elastostatics. *CMES: Computer Modeling in Engi-*

neering & Sciences, 7: 35-48.

Sellountos, E.J.; Sequeira, A.; Polyzos, D. (2009): Elastic transient analysis with MLPG (LBIE) method and local RBF's. *CMES: Computer Modeling in Engineering & Sciences*, 41: 215-241.

Sladek, J., Sladek, V., Atluri, S.N. (2000): Local boundary integral equation (LBIE) method for solving problems of elasticity with nonhomogeneous material properties. *Computational Mechanics,* **24**: 456-462.

Sladek, J., Sladek, V., Van Keer, R. (2003a): Meshless local boundary integral equation method for 2D elastodynamic problems. *Int. J. Num. Meth. Engn.*, **57**: 235-249.

Sladek, J., Sladek, V., Zhang, CH. (2003b): Application of meshless local Petrov-Galerkin (MLPG) method to elastodynamic problems in continuously nonhomogeneous solids. *CMES: Computer Modeling in Engn. & Sciences*, **4**: 637-648.

Sladek, J.; Sladek, V.; Atluri, S.N. (2004): Meshless local Petrov-Galerkin method in anisotropic elasticity. *CMES: Computer Modeling in Engineering & Sciences*, 6: 477-489.

Sladek, J.; Sladek, V.; Krivacek, J.; Zhang, Ch. (2005): Meshless Local Petrov-Galerkin Method for stress and crack analysis in 3-D axisymmteric FGM bodies, *CMES: Computer Modeling in Engineering & Sciences,* 8: 259-270.

Sladek, J.; Sladek, V.; Zhang, Ch.; Tan C.L. (2006): Meshless local Petrov-Galerkin Method for linear coupled thermoelastic analysis, *CMES: Computer Modeling in Engineering & Sciences,* 16: 57-68.

Sladek, V.; Sladek, J.; Zhang, Ch. (2008a): Computation of stresses in non-homogeneous elastic solids by local integral equation method: a comparative study. *Computational Mechanics* 41: 827-845.

Sladek, V.; Sladek, J.; Zhang, Ch. (2008b): Local integral equation formulation for axially symmetric problems involving elastic FGM. *Engineering Analysis with Boundary Elements* 32: 1012-1024.

Sladek, J.; Sladek, V.; Solek, P. (2009): Elastic analyses in 3D anisotropic functionally graded solids by the MLPG. *CMES: Computer Modeling in Engineering & Sciences* 43: 223-251.

Soares Jr., D. (2002): Time and frequency-domain dynamic analysis of non-linear models discretized by the finite element method (in Portuguese), M.Sc. Dissertation, COPPE – Federal University of Rio de Janeiro, Brazil.

Soares Jr., D. (2004): Dynamic analysis of non-linear soil–fluid–structure coupled systems by the finite element method and the boundary element method (in Portuguese), Ph.D. Thesis, COPPE – Federal University of Rio de Janeiro, Brazil.

Soares Jr., D. (2007): A time-marching scheme based on implicit Green s functions for elastodynamic analysis with the domain boundary element method. *Computational Mechanics*, **40**: 827-835.

Soares Jr., D. (2008): A time-domain FEM approach based on implicit Green s functions for the dynamic analysis of porous media. *Computer Methods in Applied Mechanics and Engineering*, **197**: 4645-4652.

Soares Jr., D. (2009): Numerical modelling of electromagnetic waves by explicit multi-level time-step FEM-BEM coupling procedures. *CMES: Computer Modeling in Engineering & Sciences*, **44**: 157-175.

Soares Jr., D., Mansur, W. J. (2003): An efficient time/frequency domain algorithm for modal analysis of non-linear models discretized by the FEM. *Computer Methods in Applied Mechanics and Engineering*, **192**: 3731-3745.

Soares Jr., D., Mansur, W. J. (2005a): A time domain FEM approach based on implicit Green's functions for non-linear dynamic analysis. *International Journal for Numerical Methods in Engineering*, **62**: 664-681.

Soares Jr., D., Mansur, W. J. (2005b): A frequency-domain FEM approach based on implicit Green's functions for non-linear dynamic analysis. *International Journal of Solids and Structures*, **42**: 6003-6014.

Soares Jr., D. ; Mansur, W.J. (2005c): An efficient time-domain BEM/FEM coupling for acoustic-elastodynamic interaction problems. *CMES: Computer Modeling in Engineering & Sciences*, **8**: 153-164.

Soares Jr., D., Mansur, W. J., Estorff, O. V. (2007): An efficient time-domain FEM/BEM coupling approach based on FEM implicit Green s functions and truncation of BEM time convolution process. *Computer Methods in Applied Mechanics and Engineering*, **196**: 1816-1826.

Soares Jr., D., Sladek, J., Sladek, V. (2009a): Time-domain analysis of elastodynamic models by meshless local Petrov-Galerkin formulations, *Advances in Boundary Element Techniques X* (eds. E. J. Sapountzakis, M.H. Aliabadi), EC Ltd., 375-380.

Soares Jr., D., Sladek, J., Sladek, V. (2009b): Non-linear dynamic analyses by meshless local Petrov–Galerkin formulations. *International Journal for Numerical Methods in Engineering*, in press (DOI: 10.1002/nme.2756).

Vavourakis, V., Sellountos, E.J., Polyzos, D. (2006): A comparison study on different MLPG (LBIE) formulatios. *CMES: Computer Modeling in Engineering & Sciences*, **13**: 171-183.